

Efficient Calculation of Modified Bessel Functions of the First Kind, $I_\nu(z)$, for Real Orders and Complex Arguments: Fortran Implementation with Double and Quadruple Precision

Mofreh R. Zaghloul^{1,2*} and Steven G. Johnson^{1†}

¹*Department of Mathematics, Massachusetts Institute of Technology,
182 Memorial Dr., Cambridge, 02139, MA, USA.

²Department of Physics, College of Sciences, United Arab Emirates
University, Al Ain, 15551, Abu Dhabi, UAE.

*Corresponding author(s). E-mail(s): m.zaghloul@uaeu.ac.ae;
mofreh_z@mit.edu;

Contributing authors: stevenj@math.mit.edu;

[†]These authors contributed equally to this work.

Abstract

We present an efficient self-contained algorithm for computing the modified Bessel function of the first kind $I_\nu(z)$, implemented in a robust Fortran code supporting double and quadruple (quad) precision. The algorithm overcomes the limitations of Algorithm 644, which is restricted to double precision and applies overly conservative underflow and overflow thresholds, leading to failures in large parameter regions. Accuracy is validated against high-precision Maple calculations, and benchmarking shows execution time reductions to 54%—80% of Algorithm 644 (in double precision). Quad precision enhances numerical stability and broadens the domain of computations, making the implementation well suited for high-precision applications in physics and engineering. This work also provides a foundation for the development of efficient algorithms for other Bessel functions.

Keywords: Modified Bessel Functions of the First Kind, Fortran Implementation, Double and Quadruple Precision

1 Introduction

The modified Bessel function of the first kind $I_\nu(z)$, also known as the hyperbolic Bessel function or Bessel function of imaginary argument [1] arises in diverse fields such as heat conduction, quantum mechanics, and signal-processing. The symbol ν is termed the order, while z is the argument. The function is defined by the integral form:

$$I_\nu(z) = \frac{1}{\pi} \int_0^\pi e^{z \cos t} \cos(\nu t) dt - \frac{\sin(\nu\pi)}{\pi} \int_0^\infty e^{-\nu t - z \cosh t} dt \quad (1)$$

where, in general, z is a complex variable, $z = x + iy$.

For $\nu = n$ (integer), the second integral disappears, i.e.

$$\begin{aligned} I_n(z) &= \frac{1}{\pi} \int_0^\pi e^{z \cos t} \cos(nt) dt \\ &= \frac{1}{\pi} \int_0^\pi e^{x \cos t} \cos nt \cos(y \cos t) dt + i \frac{1}{\pi} \int_0^\pi e^{x \cos t} \cos nt \sin(y \cos t) dt \end{aligned} \quad (2)$$

Since the advent of computers in the 1950s, numerical evaluation of Bessel functions has gained significant attention in the literature. Several researchers have addressed the challenges inherent in computing these functions, resulting in the development of various algorithms and computer codes. These efforts have addressed the problem within single and/or double precision arithmetic [2–9]. Among these, Algorithm 644 by Amos, along with its Fortran implementation, remains one of the most widely used approaches [9]. However, its applicability is inherently constrained by the limitations of double-precision arithmetic, resulting in accuracy degradation in extreme parameter regimes in addition to failures in significant regions due to overly constrained underflow/overflow thresholds.

Amos' main publication on Algorithm 644 [9] does not describe the algorithm in sufficient detail without referring to the accompanying code; however, there are also two long technical reports that describe the algorithm in much greater detail [10, 11]. Moreover, the Fortran 77 implementation of Algorithm 644, while well-established, follows an older coding style that can be difficult to interpret, modify, and extend. This makes it difficult to port the code to more modern languages and coding styles, to optimize its efficiency on more modern processors (it was initially developed for the 1960's-era CDC 6600 [10, 11]), and especially to extend the algorithm to new numeric types and floating-point precisions. The five fundamental operations in complex arithmetic are susceptible to catastrophic loss of significant digits, necessitating the use of the highest available precision when performing computations with complex numbers [12]. In this context, it may be reemphasized that many scientific and engineering applications require extensive evaluations of special functions with precision beyond the 16 significant digits typically provided by double precision arithmetic [13–16]. Among these, Bessel functions play a particularly crucial role where high-accuracy computations of these functions are essential in a wide range of fields,

including electromagnetic wave propagation, electromagnetic scattering theory, non-linear oscillator theory, plasma physics, quantum mechanics, and nuclear and particle physics. Hasegawa [17] showed that quad-precision floating-point arithmetic operation is cost-effective when some large linear systems of equations are solved by the Krylov subspace methods. While free/open-source libraries are widely available [18] for evaluating certain special functions, such as the gamma and Bessel functions, in both double and quad precision for *real* arguments, to our knowledge there is no available library for *complex*-argument Bessel functions in quad precision (as opposed to slow arbitrary-precision arithmetic). This gap highlights the pressing need for accurate and efficient implementations of Bessel functions that support quad precision, particularly for applications where round-off errors in double precision can lead to significant inaccuracies or instability. Conversely, many applications such as machine learning are driving efforts to compute in lower precision—even *half*-precision formats [19]—which makes it even more desirable to have a clear algorithmic formulation that can be easily specialized to different precisions.

Given these limitations and challenges, there is an evident need for more accessible, well-structured, and computationally efficient algorithms and implementations that support both double- and quad-precision arithmetic. The present work makes a significant contribution toward addressing this need by developing a novel approach, with a Fortran implementation, to compute modified Bessel functions of the first kind with real-order and complex arguments. Although our method shares many features with Algorithm 644, it differs in many details, especially for intermediate values of (ν, z) . The implementation is designed to run efficiently in both double- and quad-precision arithmetic, offering enhanced performance and greater adaptability to modern computational frameworks. In double precision, our implementation is at least as accurate as Algorithm 644, and is usually significantly faster (up to $2\times$, depending on ν, z). This code provides an efficient means of calculating the function with accuracies exceeding 26 significant digits in quad precision, making it not only a reliable and efficient tool for function evaluation across a range of applications, but also a robust reference for accuracy benchmarking. Furthermore, the algorithm is fully described within the following paper, as summarized in Fig. 1, including all parameters of the boundaries in (ν, z) space between different approximations.

2 Algorithm

As a first approximation, the choice of method for computing $I_\nu(z)$ depends primarily on the order ν and the magnitude of the argument $|z|$. However, in certain regions of the computational domain, the method of computation also depends on the relative magnitudes of the real and imaginary parts of z , i.e., the phase of the argument. In the following subsections, we describe the different components of the present algorithm and their applicability across various parameter regimes. For clarity and reference, Figure 1 provides an overview of the regions and methods employed in the computation of $I_\nu(z)$.

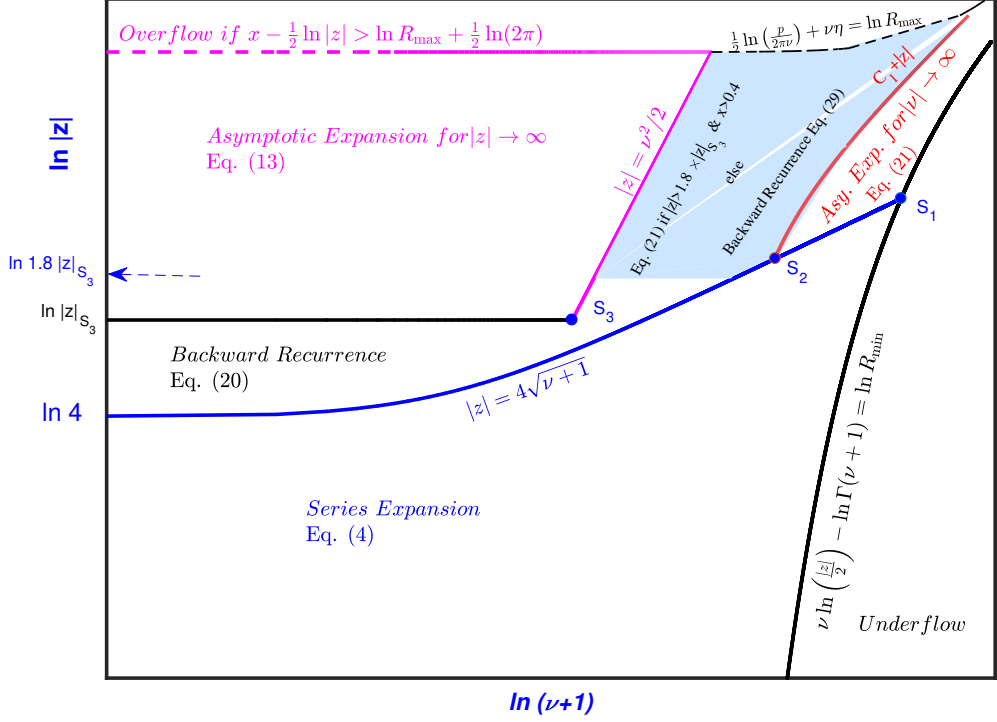


Fig. 1: Schematic computational regions and corresponding methods used in the present algorithm. Specific numerical values of the points S_1 , S_2 , and S_3 are summarized in Table A in the appendix.

2.1 Small z : Power Series Expansion

The series representation of the modified Bessel function of the first kind, $I_\nu(z)$, originates from the Frobenius method to solve the the modified Bessel function:

$$z^2 \frac{d^2 y}{dz^2} + z \frac{dy}{dz} - (z^2 + \nu^2)y = 0 \quad (3)$$

It provides an alternative expression that is particularly useful for analytical and computational purposes where [20, 21].

$$I_\nu(z) = \left(\frac{z}{2}\right)^\nu \sum_{k=0}^{\infty} \frac{\left(\frac{z^2}{4}\right)^k}{\Gamma(k + \nu + 1)k!} = \frac{\left(\frac{z}{2}\right)^\nu}{\Gamma(\nu + 1)} \sum_{k=0}^{\infty} \frac{\left(\frac{z^2}{4}\right)^k \Gamma(\nu + 1)}{\Gamma(k + \nu + 1)k!} \quad (4)$$

This series converges for all finite values of z , which means that it is valid for any z . However, in practical computation, the rate of convergence depends on z and ν . For small z , the series converges rapidly, making it highly efficient for numerical evaluation. Algorithm 644 uses this series to efficiently calculate the function for the region $|z| \leq$

$2\sqrt{\nu+1}$. In the present algorithm, we evaluate the series recursively for the broader region $|z| \leq 4\sqrt{\nu+1}$, as:

$$I_\nu(z) = \frac{\left(\frac{z}{2}\right)^\nu}{\Gamma(\nu+1)} \left[\sum_{k=0}^{\infty} T_k \right], \quad (5)$$

where the recurrence relation for T_k is given by:

$$T_0 = 1, \quad T_{k+1} = \frac{\left(\frac{z^2}{4}\right)}{(k+1)(k+\nu+1)} T_k, \quad k = 0, 1, 2, \dots \quad (6)$$

Expanding the region of applicability of this series in the present algorithm enhances its efficiency (as demonstrated by the benchmarks below), as evaluating points in the newly included region using the series expansion is more efficient than employing backward recurrence or other methods used in Algorithm 644.

The series summation can be terminated at $k = K$ when the relative contribution of the last term satisfies:

$$\frac{|T_K|}{\left| \sum_{k=0}^{K-1} T_k \right|} < \epsilon, \quad (7)$$

where ϵ is a predetermined tolerance (mostly taken to be the spacing of floating point numbers in the precision arithmetic used).

Alternatively, a more restrictive condition for truncating the series, as employed in Algorithm 644, can be established by comparing the relative contribution of the last term to the $k = 1$ term, given by:

$$\frac{|\bar{T}_{k+1}|}{\left| \frac{(z^2/4)}{(\nu+1)} \right|} < \epsilon, \quad (8)$$

For values of $|z| \leq 4\sqrt{\nu+1}$, where the series in Eq. (4) converges efficiently and can be used for function evaluation, the pre-sum factor may undergo underflow when:

$$\nu \ln \left(\frac{|z|}{2} \right) - \ln \Gamma(\nu+1) < \ln R_{\min} \quad (9)$$

where R_{\min} is the smallest positive normalized floating-point number. This condition applies for $\nu \neq 0$, as for $\nu = 0$, the pre-sum factor remains unity and never underflows. When this underflow condition is met, the series evaluation should be skipped and the function should be set to $I_\nu(z) = (0.0, 0.0)$.

Underflow in either the real or imaginary part of the pre-sum term is also possible. However, as long as at least one component remains nonzero, the computation may proceed.

The underflow condition in Eq. (9), combined with the applicability condition of the series expansion in Eq. (4), namely $|z| \leq 4\sqrt{\nu+1}$, can be solved using a zero

search algorithm to determine the terminal point (point of intersection) S_1 in Fig. 1. Beyond this point, i.e., for $|z| > |z|_{S_1}$ and $\nu > \nu_{S_1}$, the series expansion becomes either numerically inefficient or undergoes underflow.

2.2 Asymptotic Expansion for Large Argument $z \rightarrow \infty$

The asymptotic expansion of the modified Bessel function of the first kind, $I_\nu(z)$, for a large argument $z \rightarrow \infty$ is an important tool for numerical computations, especially when z is much larger than ν . This expansion allows for an efficient and accurate evaluation of $I_\nu(z)$ in the region where

$$|z| \geq \max(|z|_{S_3}, \nu^2/2) \quad (10)$$

The value of $|z|_{S_3}$ is precision dependent and is determined by experiments. For double precision, the value used by Algorithm 644 is

$$|z|_{S_3} = 1.2D + 2.4 \approx 21.6 \quad (11)$$

where D is the number of decimal digits in the precision used (≈ 16 for double precision). Our experiments showed that this boundary can be further lowered while maintaining the same level of accuracy, leading to an improvement in efficiency. In this case, $|z|_{S_3}$ can be expressed as:

$$|z|_{S_3} = \begin{cases} 16.0 & \text{double precision} \\ 60.0 & \text{quad precision} \end{cases} \dots \quad (12)$$

For $|z| \geq |z|_{S_3}$ and $|z| > \nu^2/2$, the asymptotic expansion for large $z \rightarrow \infty$ with fixed ν [22] is given by:

$$I_\nu(z) \approx \frac{e^z}{(2\pi z)^{1/2}} \sum_{k=0}^{\infty} \frac{(-1)^k a_k(\nu)}{z^k} + e^{\pm(\nu+1/2)\pi i} \frac{e^{-z}}{(2\pi z)^{1/2}} \sum_{k=0}^{\infty} \frac{a_k(\nu)}{z^k}, \quad (13)$$

$$-\pi + \delta \leq \arg z \leq \pi - \delta$$

where

$$a_k(\nu) = \frac{(4\nu^2 - 1^2)(4\nu^2 - 3^2) \dots (4\nu^2 - (2k-1)^2)}{k! 8^k} \quad (14)$$

Equation (13) can be computed recursively:

$$I_\nu(z) \approx \frac{e^z}{(2\pi z)^{1/2}} \sum_{k=0}^{\infty} (-1)^k T_k + e^{\pm(\nu+1/2)\pi i} \frac{e^{-z}}{(2\pi z)^{1/2}} \sum_{k=0}^{\infty} T_k, \quad (15)$$

$$-\pi + \delta \leq \arg z \leq \pi - \delta$$

with

$$T_0 = 1, \quad T_{k+1} = \frac{(4\nu^2 - (2k+1)^2)}{8(k+1)z} T_k, \quad k \geq 0 \quad (16)$$

A sufficient condition for convergence is:

$$\frac{T_{k+1}}{T_k} = \frac{4\nu^2 - (2k+1)^2}{8(k+1)z} \leq 1 \quad (17)$$

This ratio decreases as k increases, implying that for large z , the series converges if $|z| > \nu^2/2$.

The summations in Eq. (15) terminate after a maximum number of terms, similar to the approach used with the small z series expansion. However, overflow may occur when:

$$\left| \ln \frac{e^z}{(2\pi z)^{1/2}} \right| > \ln R_{\max} \quad (18)$$

or equivalently:

$$x - \frac{1}{2} \ln |z| > \ln R_{\max} + \frac{1}{2} \ln(2\pi) \quad (19)$$

As seen from Eq. (19), the overflow in this part of the computational domain depends on the angle or phase of the complex variable z , which means that there is no well-defined single-value boundary for overflow in the plane $\nu - |z|$. The dashed line in Fig. 1, therefore, represents a symbolic boundary rather than a strict mathematical limit.

For the special case of a real argument $z = x$, the inequality in (19) is solved using a zero search routine, showing that overflow occurs when $x > 713.9871$ for double precision and $x > 11360.7249$ for quad precision arithmetic.

2.3 Intermediate Region

The two approaches discussed in Sections 2.1 and 2.2 share similarities with Algorithm 644, particularly in their general framework. However, the present algorithm introduces modifications to the selection of the boundary to enhance computational efficiency. A key distinction arises in the treatment of the intermediate region within the computational domain. While Algorithm 644 employs both Miller's algorithm for backward recurrence and the Wronskian relation in this region, the present approach adopts a different strategy, leading to a number of significant differences.

The use of the Wronskian relation in Algorithm 644 requires the computation of the modified Bessel functions of the second kind; namely $K_\nu(z)$ and $K_{\nu+1}(z)$, introducing additional dependencies. Specifically, the Wronskian relation for modified Bessel functions of the first and second kinds is given by

$$I_\nu(z)K_{\nu+1}(z) + I_{\nu+1}(z)K_\nu(z) = \frac{1}{z}. \quad (20)$$

Since the computation of $K_\nu(z)$ is necessary in this approach, relying on the Wronskian relation makes the evaluation of $I_\nu(z)$ not entirely self-contained. In contrast, the present algorithm is designed to compute $I_\nu(z)$ directly, eliminating the need for external evaluations of $K_\nu(z)$, thereby improving both efficiency and independence from additional special function computations.

2.3.1 Asymptotics for Large Orders ($\nu \rightarrow \infty$) & Arguments

Asymptotic expansion provides a powerful method for approximating special functions, particularly in regimes where standard series expansions become inefficient or exhibit convergence and/or stability issues. In the case of the modified Bessel function of the first kind, such expansions are essential for ensuring accuracy across a broad range of ν and z .

The asymptotic behavior of $I_\nu(\nu z)$ for large ν and varying arguments z necessitates an expansion, expressed in terms of scaled variables and functions such as p and η , that ensures a consistent and computationally efficient representation even when z is near the turning points of the function [21, 23].

The asymptotic expansion of $I_\nu(\nu z)$ is expressed as $\nu \rightarrow \infty$ through the positive real values as [22];

$$I_\nu(\nu z) \approx \left(\frac{p}{2\pi\nu}\right)^{1/2} e^{\nu\eta} \left(1 + \sum_{k=1}^{\infty} \frac{U_k(p)}{\nu^k}\right) \quad (21)$$

where p and η are scaling functions depending on z . These functions are defined as:

$$p = (1 + z^2)^{-1/2} \quad (22)$$

$$\eta = p^{-1} + \ln\left(\frac{pz}{p+1}\right) \quad (23)$$

The coefficients $U_k(p)$ refine the approximation through a recursive relationship:

$$U_{k+1}(p) = \frac{1}{2}p^2(1-p^2)U_k'(p) + \frac{1}{8}\int_0^p (1-5t^2)U_k(t) dt, \quad U_0 = 1 \quad (24)$$

This recursive formulation allows for higher-order corrections, enhancing the accuracy of the expansion in practical computations. Asymptotic expansion is particularly advantageous for numerical computation of $I_\nu(\nu z)$, as it mitigates numerical instabilities associated with traditional series expansions. The coefficients $U_k(p)$ can be precomputed and stored for efficient evaluation.

A threshold for employing this asymptotic expansion in the present algorithm was empirically determined through numerical experiments, where the results were compared with the reference values generated using the Maple software package [24]. The threshold is expressed as:

$$\nu_{\text{th}}(|z|) = C_1 + |z| \quad (25)$$

where C_1 is a constant that generally depends on the precision arithmetic used for the computations and $|z|$ denotes the magnitude of the argument z .

The series for the asymptotic expansion can also be regarded as a generalized asymptotic expansion to approximate the function when both $|z|$ and ν are large. Conventionally, the accuracy of this expansion is expected to deteriorate near the Stokes lines, which occur at $\arg z = \pm\pi/3$ and $\arg z = \pm\pi$. This behavior is associated with

the Stokes phenomenon, where exponentially subdominant terms begin to contribute significantly, leading to deviations from the asymptotic approximation. Thus, expansion is typically recommended for use in the sector where $\arg z < \pi/3$, which in terms of the real and imaginary components of z , translates to the condition

$$|y| < \sqrt{3}|x| \quad (26)$$

However, our empirical investigations suggest that this theoretical constraint is conservative. The computational results indicate that for sufficiently large $|z|$, this asymptotic expansion remains accurate beyond the classical boundary given by Eq. (26). For example, when using double precision, it was found that asymptotic expression remains accurate for $|z| \geq 28$ and $|y| < 2.5|x|$, and for $|z| \geq 50.53$ and $|y| < 5.0|x|$, etc. This observation suggests that the onset of Stokes switching, while theoretically expected near $\arg z = \pm\pi/3$, is not an abrupt transition. Instead, the dominance of the leading-order asymptotic terms for large $|z|$ delays the breakdown of the expansion, effectively extending its region of applicability. Moreover, the presence of a sufficiently large real component x appears to stabilize the expansion, mitigating the growth of subdominant terms that would otherwise introduce inaccuracies.

It should be noted that such dependence on $\arg z$ disappears for very large values of the order ν . Accordingly, the accuracy of the asymptotic expansion in Eq. (21) depends on both the magnitude and the phase of the complex argument z together with the order ν .

A suitable value for the empirical constant C_1 in Eq. (25) has been determined as

$$C_1 = \begin{cases} 52.0 & \text{double precision} \\ 262.0 & \text{quad precision} \end{cases}. \quad (27)$$

Furthermore, the expression in Eq. (21) is extended beyond the threshold in Eq. (25) to the intermediate region, where

$$|z| > \begin{cases} 28.8 & \text{double precision} \\ 180.0 & \text{quad precision} \end{cases} \quad \text{and} \quad x > 0.4 \times y. \quad (28)$$

(It should be noted that all such empirical numerical thresholds presented in our algorithm are chosen to work well, but we do not claim that they are strictly optimal; they could be further fine-tuned.)

2.3.2 Backward Recurrence

For the remaining part of the intermediate region that is not covered by the asymptotic expansion for $\nu \rightarrow \infty$ or its extension to the large- z , large- ν region, the function can be evaluated using the stable backward recurrence relation:

$$I_{\nu-1}(z) = \frac{2\nu}{z} I_{\nu}(z) + I_{\nu+1}(z) \quad (29)$$

In order to employ this recurrence, the key question is what terminal order ν_{term} to use, and what corresponding values of $I_{\nu_{\text{term}}}$ and $I_{\nu_{\text{term}}+1}$. Algorithm 644 employs Miller’s method [7], which uses a very large ν_{term} for which $I_{\nu_{\text{term}}+1} \approx 0$ and $I_{\nu_{\text{term}}}$ can simply be set to 1, necessitating a subsequent renormalization step. In contrast, we choose a much smaller ν_{term} , and compute $I_{\nu_{\text{term}}}$ and $I_{\nu_{\text{term}}+1}$ explicitly using a series or asymptotic expansion. In particular, we define ν_{term} as:

$$\nu_{\text{term}} = \begin{cases} \lfloor |z|^2/16 \rfloor + (\nu - \lfloor \nu \rfloor), & \text{for } 4\sqrt{\nu+1} < |z| < |z|_{S_2}, \\ \nu_{\text{th}}(|z|), & \text{otherwise.} \end{cases}, \quad (30)$$

where ν_{th} is given by Eq. (25). The values of $I_{\nu_{\text{term}}}(z)$ and $I_{\nu_{\text{term}}+1}(z)$ are then calculated using the series expansion in Eq. (4) if $|z| < |z|_{S_3}$; otherwise, the asymptotic expansion Eq. (21) for $\nu \rightarrow \infty$ is used. This approach eliminates the difficulties associated with selecting an excessively large terminal order and determining a suitable, computationally efficient normalization factor, which are common challenges in the Miller method.

3 Implementation and Accuracy Verification

The algorithm outlined in Section 2 has been implemented as a Fortran module that supports double- and quad-precision arithmetic. The precision level is controlled by an integer parameter, `rk`, which specifies the real kind for both the main module and the driver code. This parameter is defined in a subsidiary module, `set_rk`.

To verify accuracy and benchmark the efficiency of the present algorithm for computing the modified Bessel functions of the first kind, we conducted a detailed comparison against Algorithm 644, a widely recognized Fortran implementation operating in double-precision arithmetic. To the best of the authors’ knowledge, no existing free/open-source implementation of complex-argument Bessel functions (in Fortran or other compiled languages) is specifically designed for quad-precision arithmetic (as opposed to libraries in arbitrary precision arithmetic).

For accuracy assessment, high-precision reference data were generated using Maple’s arbitrary-precision implementation, additionally cross-checked with the arbitrary-precision mpmath library [25], ensuring a reliable basis for error evaluation. The relative errors between the computed values from both algorithms and the Maple-generated reference values were analyzed over a broad range of parameters, encompassing both small and large orders and arguments. This comprehensive evaluation confirms the robustness of the present algorithm under practical conditions. Additionally, the performance comparison with Algorithm 644 highlights the superior efficiency of the proposed algorithm and its implementation.

3.1 Accuracy Verification: Double Precision

To assess accuracy in double precision, we employed a grid of 283,254 points distributed predominantly uniformly on a logarithmic scale in the ν - $|z|$ domain, along with 2,648 additional special points positioned near the boundaries of the algorithm’s computational regions, as illustrated in Fig. 1. These special points are critical for

evaluating numerical stability and accuracy near regions' transitions. Figure 2 depicts the full grid, including the special points near the boundary of the region.

All function values at these test points were computed using high-precision Maple calculations, ensuring that they fall within the range of representable floating-point numbers in double-precision arithmetic.

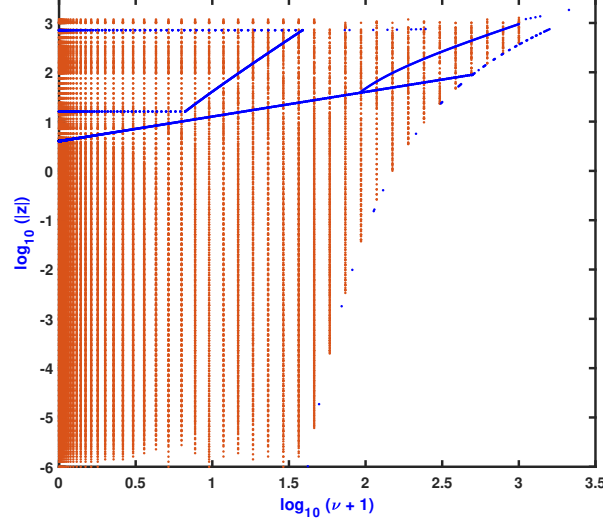


Fig. 2: The grid of tested points using double-precision arithmetic, along with additional points superimposed on or near the boundaries of the regions defined in the present algorithm, as shown in Fig. 1. Maple calculations for these input points fall within the range of representable floating-point real numbers in double-precision arithmetic.

Figure 3 presents 2D colormap plots of the base-10 logarithm of the ratio of the relative error $|\text{computed} - \text{reference}|/|\text{reference}|$ in calculating either the real part (a) or imaginary part (b) of $I_\nu(z)$ of the dataset points tested using the present algorithm, divided by the corresponding relative error of Algorithm-644, with Maple calculations as the reference.

Algorithm 644 skips computations and returns an error code over a significant portion of the computational domain due to overly conservative underflow/overflow thresholds. These regions, where Algorithm 644 fails to perform calculations, extend several orders of magnitude before reaching the actual underflow/overflow limits. For such regions, Algorithm 644 returns (0.0, 0.0), resulting in a 100% relative error, as indicated by the red regions (indicating an extremely small relative error ratio) in parts (a) and (b) of Fig. 3. However, the present algorithm remains capable of computing the function with high accuracy in these challenging regions. For reference, a sample of points from these regions is provided in Table 1.

Insert table 1 here

Away from these regions where Algorithm 644 fails due to overly conservative underflow/overflow thresholds, the accuracy of both algorithms is comparable.

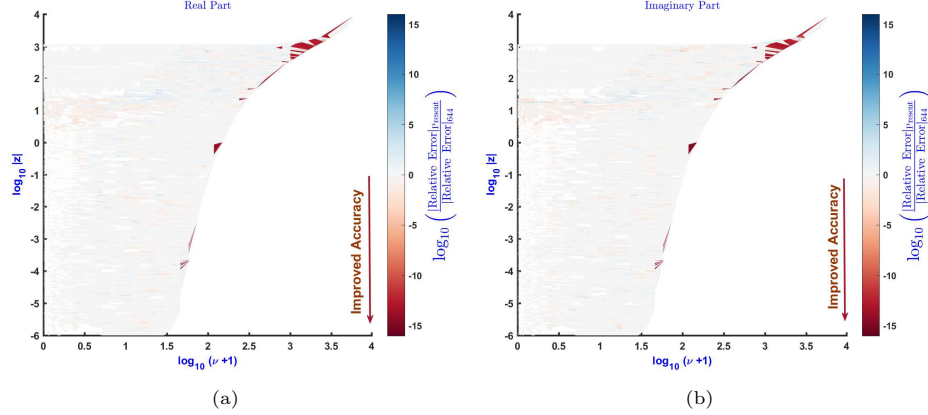


Fig. 3: Colormap plots of the base-10 logarithm of the ratio of the relative error in calculating the real part (a) and imaginary part (b) of $I_\nu(z)$ of the dataset points tested using the present algorithm relative to Algorithm-644, with Maple calculations as the reference.

3.2 Accuracy Verification: Quad Precision

The limitations in both the computational domain and accuracy, as discussed in Section 3.1, stem primarily from the constraints of double precision arithmetic (approximately 16 significant digits). These constraints suggest that higher precision may be required to achieve greater accuracy and to extend the computational domain of the function, particularly for large orders and arguments where numerical instabilities become significant. Although enormous accuracy and range can be obtained using arbitrary-precision arithmetic (e.g. in Maple or mpmath), performance is substantially improved by using quad precision support in a compiled language (such as Fortran).

A new grid of points in the expanded ν - $|z|$ domain is employed to verify the accuracy of the quad-precision implementation. This grid, along with specially selected points located on or near the boundaries of the computational regions of the present algorithm, comprises a total of 280,636 points, as illustrated in Fig. 4. Compared to the computational domain used for double-precision calculations, the quad-precision domain extends a few orders of magnitude in both order and argument.

Figure 5 presents 2D colormap plots of the relative error in computing the real part (a) and imaginary part (b) of $I_\nu(z)$ for the newly expanded grid of input data points used in quad-precision calculations, including selected points on or near region boundaries. Again, high-precision Maple results were used as the reference. As shown in the figure, the present Fortran implementation achieves high accuracy, with errors on the order of $\approx 10^{-27}$ for the real part and $\approx 10^{-26}$ for the imaginary part.

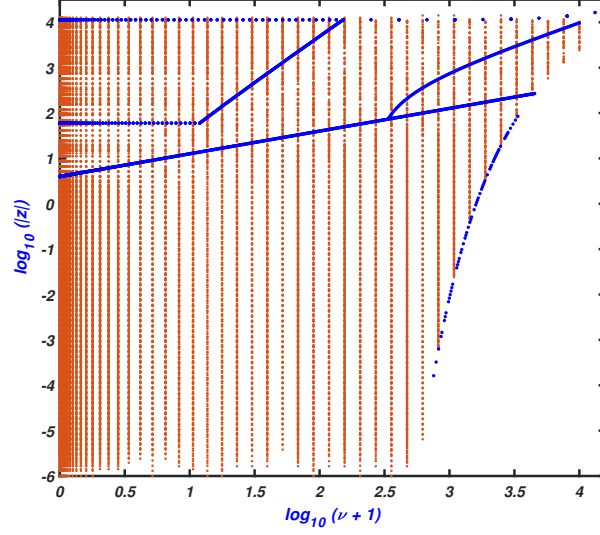


Fig. 4: The grid of tested points using quad-precision arithmetic, along with superimposed points on or near the borders of the regions in the present algorithm, as shown in Fig. 1. Maple calculations for these input points fall within the range of the minimum and maximum floating-point real numbers in quad-precision arithmetic.

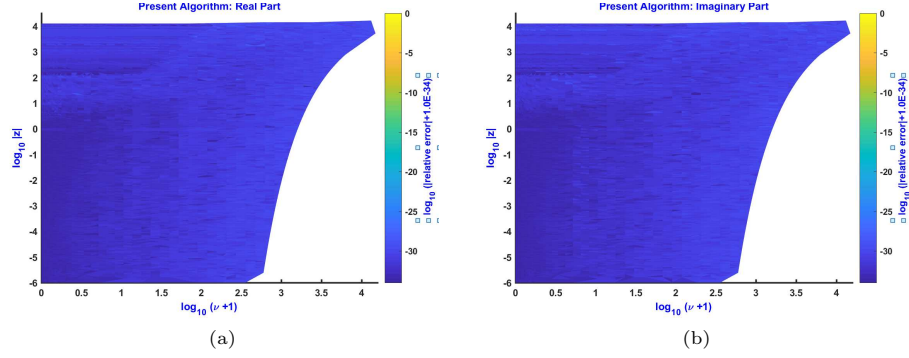


Fig. 5: Colormap plots of the relative error in calculating the real part (a) and imaginary part (b) of $I_\nu(z)$ for the dataset points tested using the present algorithm, with Maple calculations as the reference.

4 Efficiency Benchmarking: Present Algorithm vs Algorithm 644

To evaluate the computational efficiency of the present algorithm, a systematic benchmarking comparison is performed against Algorithm 644. The benchmarking uses the extensive dataset described in Section 3.1, ensuring a thorough and comprehensive assessment.

Execution times are measured for both algorithms under identical computational conditions, allowing for a direct and fair performance comparison. Since Algorithm 644 was designed primarily for double precision and does not support quad precision, efficiency tests for the present algorithm are conducted exclusively in double precision. This evaluation highlights the computational advantages of the new algorithm, particularly in terms of its superior execution speed, support for quad precision, and robustness in computational domains with extreme parameter values where Algorithm 644 fails.

Efficiency tests are conducted using the same set of test points previously used for double-precision accuracy verification. Each test consists computing all points 50 times and is repeated 21 times. To minimize noise from system-level fluctuations, the shortest execution time is recorded out of all 21 repetitions [26]. Time was measured using the `SYSTEM_CLOCK` function, which corresponds to the high-resolution `QueryPerformanceCounter` system call in GNU Fortran, in order to resolve short times for the point-by-point calculations.

Benchmarking experiments are conducted under controlled conditions using a fixed hardware environment with minimal background processes. The following Fortran compilers are tested:

- GNU Fortran (i686-posix-dwarf-rev0, Built by MinGW-W64 project) 8.1.0,
- GNU Fortran (Rev3, Built by MSYS2 Project) 12.1.0,

- NAG Fortran Compiler Release 7.1 (Hanzomon) Build 7110,
- Intel(R) Fortran Intel(R) 64 Version 2021.9.0 Build 20230302_000000,
- IFX (LLVM-based), from Intel(R) Fortran 64 Version 2021.9.0.

All tests are compiled using standard optimization flags (`-O3`, `-O2`, `-O1`, and `-O0`) to assess the impact of compiler optimizations. The benchmark results are reported with attention to reproducibility and system specifications are documented accordingly.

In addition to evaluating execution time over the entire dataset, experiments are conducted for individual sub-regions depicted in Fig. 1. The summarized results, presented in Table 2, indicate that the present algorithm consistently outperforms Algorithm 644 across the entire domain and within each sub-region, regardless of the compiler used or level of optimization. Expressed as a percentage of the computational time required by Algorithm 644, the present algorithm achieves execution times ranging between 53% and 77% of those recorded for Algorithm 644, depending on the compiler and optimization level. The overall average execution time per point is on the order of tenths of a microsecond.

Further insight can be gained by analyzing the computational time at each individual point, rather than averaged over the entire domain or sub-regions. Figure 6(a) shows a colormap of the base-10 logarithm of the execution time (in μs) for a single evaluation. The shown time represents the shortest recorded computation time across multiple experiments. Figure 6(b) displays the base-10 logarithm of the execution time ratio comparing the present algorithm to Algorithm 644 at each point within the computational domain.

While the present algorithm exhibits superior performance across most of the computational domain—both in overall execution time and within specific sub-regions—there exist small regions or isolated points where Algorithm 644 executes faster. Some of these points are located on or near the underflow boundary, where Algorithm 644 entirely bypasses computations. However, other points or small isolated regions within the computational domain primarily correspond to extremely high-order, extremely high-argument values, suggesting potential avenues for further optimization.

As observed in Fig. 6(b), the efficiency improvement is particularly pronounced in the backward recurrence region, where the present algorithm employs direct absolute backward recurrence. In contrast, Algorithm 644 relies on Miller’s algorithm and the Wronskian relation, necessitating the computation of modified Bessel functions of the second kind, thereby introducing additional dependencies. In addition, a noticeable improvement in efficiency can also be observed in the small z region and the $|z| \rightarrow \infty$ region.

It is worth noting that the average execution time per evaluation using quad precision is a few μs , which is approximately an order of magnitude slower than double precision.

Table 2: Execution time taken by the present algorithm relative to that taken by Algorithm 644 for computing the dataset described in Fig. 2 using double-precision arithmetic. Computations were performed using the five Fortran compilers described above on an Intel® Core™ i7-6600U CPU @ 2.60 GHz, 2.81 GHz processor.

Region	Small $ z $	As. $z \rightarrow \infty$	As. $\nu \rightarrow \infty$	BkWd Rec.	All
GNU Fortran (i686-posix-dwarf-rev0, Built by MinGW-W64 project) 8.1.0					
Gfortran -O3	54.9%	56.3%	54.0%	50.8%	53.6%
Gfortran -O2	55.0%	54.1%	50.7%	50.7%	53.7%
Gfortran -O1	55.4%	56.8%	54.5%	51.1%	54.0%
Gfortran -O0	53.6%	57.4%	53.9%	51.2%	53.7%
GNU Fortran (Rev3, Built by MSYS2 Project) 12.1.0					
Gfortran -O3	70.9%	74.9%	72.7%	71.9%	73.0%
Gfortran -O2	71.0%	74.7%	72.4%	71.5%	72.9%
Gfortran -O1	69.7%	73.5%	71.7%	70.3%	71.3%
Gfortran -O0	61.7%	66.5%	63.3%	61.7%	65.0%
NAG Fortran Compiler Release 7.1 (Hanzomon) Build 7110					
Nagfor -O3	62.8%	67.7%	63.9%	61.8%	64.7%
Nagfor -O2	63.4%	68.6%	64.7%	63.1%	65.7%
Nagfor -O1	64.1%	71.2%	66.2%	64.2%	67.1%
Nagfor -O0	54.0%	59.4%	55.1%	53.5%	56.3%
Intel(R) Fortran Intel(R) 64 Version 2021.9.0 Build 20230302_000000					
Ifort -O3	74.6%	82.5%	78.4%	79.8%	79.6%
Ifort -O2	74.7%	82.5%	78.1%	79.5%	78.8%
Ifort -O1	72.2%	81.0%	76.7%	76.5%	77.3%
Ifort -O0	74.6%	82.8%	77.9%	79.1%	78.2%
IFX (LLVM-based), from Intel® Fortran 64 Version 2021.9.0					
IFX -O3	72.1%	76.2%	73.6%	73.8%	73.4%
IFX -O2	72.0%	77.4%	73.6%	74.6%	73.4%
IFX -O1	69.1%	74.9%	71.2%	72.3%	70.9%
IFX -O0	72.3%	77.2%	73.9%	74.4%	74.0%

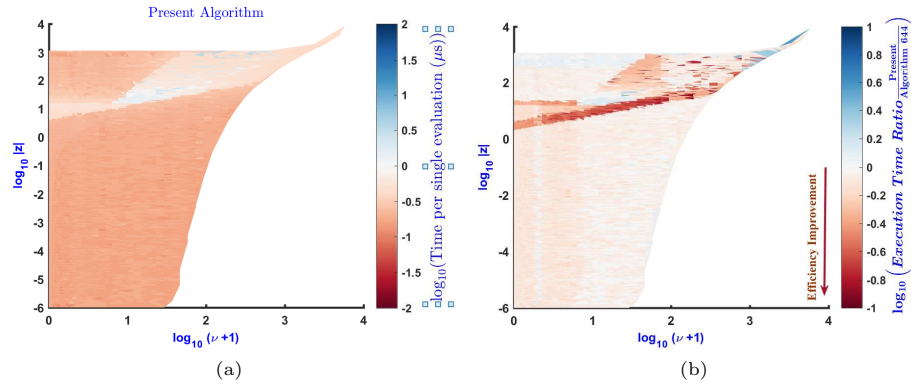


Fig. 6: Two-dimensional colormap plots of the base-10 logarithm of: (a) execution time per evaluation (in μs) of the present algorithm, and (b) the time ratio of the present algorithm to Algorithm 644 across the domain. Computations used an Intel® Core™ i7-6600U CPU @ 2.60–2.81 GHz with GNU Fortran 12.1.0 (Rev3, MSYS2) with optimization level -O3.

5 Conclusions

This work introduces a robust and highly efficient algorithm and Fortran implementation for computing the modified Bessel functions of the first kind, $I_\nu(z)$, supporting both double- and quad-precision arithmetic. The implementation overcomes critical limitations in existing algorithms, particularly Algorithm 644, by extending the computational domain to cover regions where Algorithm 644 fails due to its overly restrictive underflow and overflow conditions. Extensive accuracy verification against high-precision Maple calculations confirms that the present algorithm maintains high fidelity across a broad range of input values, with relative errors as low as $\lesssim 10^{-26}$ in quad precision.

A comprehensive efficiency benchmarking study further highlights the advantages of the present implementation, demonstrating its computational superiority over Algorithm 644 across all tested compilers and optimization levels. Execution times are consistently reduced, making the algorithm particularly valuable for large-scale simulations and high-performance computing tasks. The introduction of quad-precision support addresses the growing demand for increased numerical stability in scientific disciplines such as high-energy physics, astrophysics, and quantum mechanics.

By providing an accurate, efficient, and versatile computational tool, this work not only establishes a new standard for computing $I_\nu(z)$ with improved accuracy and efficiency but also lays the foundation for future extensions to other families of Bessel functions. It is important to note that the results and conclusions presented in this study are based on the tested dataset and the specifics of the compilers and hardware configurations used herein. Variations in computational environments may lead to differences in performance and numerical behavior. As part of our ongoing efforts, this approach will be further refined to encompass the complete spectrum of Bessel functions, ensuring a comprehensive and high-performance computational framework for diverse scientific and engineering applications. Moreover, our algorithms are presented in a well-document form that is easily adaptable to other precisions in widespread use besides double and quadruple—such as optimizing for lower (single and half) precision, or different high-precision formats such as octuple, double-double, and quad-double formats—mainly, one needs to simply re-tune a few empirical constants in equations (12, 27, 28).

Acknowledgment

This work is supported by UAE University UPAR research grants **G00004187 (2022)** and **G00004995 (2024)**.

Appendix

Table A: Specific values for the points S1, S2, and S3 in Fig. 1 as used in the present algorithm, for IEEE double and quadruple precisions.

Point	ν (double)	$ z $ (double)	ν (quad)	$ z $ (quad)
S1	498.85	89.43	4514.29	268.78
S2	91.46	38.46	336.48	73.48
S3	52.0	16.0	262.0	60.0

Declaration of Interests

☒ The authors declare that they have no known competing financial interests or personal relationships that could have appeared to influence the work reported in this paper.

☐ The authors declare the following financial interests/personal relationships which may be considered as potential competing interests:

Funding

This work is supported by the UAE University UPAR research grants **G00004187 (2022)** and **G00004995 (2024)**.

Conflict of interest/Competing interests

We are not aware of any.

Code availability

Upon final acceptance, the Fortran code and associated data files will be deposited in the GitHub open-access repository.

Author contribution

Authors contributed equally to the manuscript.

References

- [1] Oldham, K., Myland, J., Spanier, J.: An Atlas of Functions: With Equator, the Atlas Function Calculator, 2nd edn. Springer, New York, NY (2009)
- [2] Temme, N.M.: On the numerical evaluation of the modified Bessel function of the third kind. *Journal of Computational Physics* **19**(3), 324–337 (1975) [https://doi.org/10.1016/0021-9991\(75\)90082-0](https://doi.org/10.1016/0021-9991(75)90082-0)
- [3] Barnett, A.R.: The Calculation of Spherical Bessel and Coulomb Functions, pp. 181–202. Springer, New York, NY (1996). https://doi.org/10.1007/978-3-642-61010-3_9
- [4] Amos, D.E., Daniel, S.L., Weston, M.K.: Algorithm 511: CDC 6600 subroutines IBESS and JBESS for Bessel functions $I_\nu(x)$ and $J_\nu(x)$, $x \geq 0$, $\nu \geq 0$. *ACM Transactions on Mathematical Software* **3**(1), 93–95 (1977) <https://doi.org/10.1145/355719.355727>
- [5] Amos, D.E.: Erratum: Algorithm 511: CDC 6600 subroutines IBESS and JBESS for Bessel functions $I_\nu(x)$ and $J_\nu(x)$, $x \geq 0$, $\nu \geq 0$. *ACM Transactions on Mathematical Software* **4**(4), 411 (1978) <https://doi.org/10.1145/356502.356501>
- [6] Amos, D.E.: Algorithm 556: Exponential integrals. *ACM Transactions on Mathematical Software* **6**(3), 420–428 (1980) <https://doi.org/10.1145/355900.355913>
- [7] Zhang, S., Jin, J.-M.: *Computation of Special Functions*. Wiley, Hoboken, NJ (1996)
- [8] MacLeod, A.J.: Algorithm 757: MISCFUN, a software package to compute uncommon special functions. *ACM Transactions on Mathematical Software* **22**(3), 288–301 (1996) <https://doi.org/10.1145/232826.232846>
- [9] Amos, D.E.: Algorithm 644: A portable package for Bessel functions of a complex argument and nonnegative order. *ACM Transactions on Mathematical Software* **12**(3), 265–273 (1986) <https://doi.org/10.1145/7921.214331>
- [10] Amos, D.E.: Computation of Bessel functions of complex argument. Technical Report SAND83-0086, Sandia National Laboratories, Albuquerque, NM (1983)
- [11] Amos, D.E.: Computation of Bessel functions of complex argument and large order. Technical Report SAND83-0643, Sandia National Laboratories, Albuquerque, NM (1983)
- [12] Beebe, N.H.F.: *The Mathematical-Function Computation Handbook: Programming Using the MathCW Portable Software Library*, p. 1114. Springer, New York, NY (2017). <https://doi.org/10.1007/978-3-319-64110-2>

- [13] Zaghloul, M.R.: Efficient multiple-precision computation of the scaled complementary error function and the Dawson integral. *Numerical Algorithms* **95**(3), 1291–1308 (2023) <https://doi.org/10.1007/s11075-023-01608-8>
- [14] Zaghloul, M.R., Alrawas, L.: Calculation of Fresnel integrals of real and complex arguments up to 28 significant digits. *Numerical Algorithms* **96**(2), 489–506 (2023) <https://doi.org/10.1007/s11075-023-01654-2>
- [15] Zaghloul, M.R.: Efficient numerical algorithms for multi-precision and multi-accuracy calculation of the error functions and Dawson integral with complex arguments. *Numerical Algorithms* **97**(2), 869–887 (2024) <https://doi.org/10.1007/s11075-023-01727-2>
- [16] Mukunoki, D., Takahashi, D.: Implementation and evaluation of quadruple precision BLAS functions on GPUs. In: *Applied Parallel and Scientific Computing. Lecture Notes in Computer Science*, vol. 7133, pp. 249–259. Springer, ??? (2012). https://doi.org/10.1007/978-3-642-28151-8_25
- [17] Hasegawa, H.: Utilizing the quadruple-precision floating-point arithmetic operation for the Krylov subspace methods. In: *Proceedings of the SIAM Conference on Applied Mathematics*. Society for Industrial and Applied Mathematics (SIAM), Los Angeles, CA (2003). Presented at the SIAM Conference on Applied Mathematics, July 2003
- [18] Coudert, F.-X., et al.: libquadmath: The GCC Quad-Precision Math Library. (2010). <https://gcc.gnu.org/onlinedocs/libquadmath/>
- [19] Cherubin, S., Agosta, G.: Tools for reduced precision computation: A survey. *ACM Computing Surveys* **53**(2), 1–35 (2020) <https://doi.org/10.1145/3381039>
- [20] Abramowitz, M., Stegun, I.A.: *Handbook of Mathematical Functions: with Formulas, Graphs, and Mathematical Tables*. Dover, New York, NY (1964)
- [21] Olver, F.W., Lozier, D.W., Boisvert, R., Clark, C.W.: *The NIST Handbook of Mathematical Functions*. Cambridge University Press, New York, NY (2010)
- [22] Standards, N.I., (NIST)., T.: *Digital Library of Mathematical Functions*. <https://dlmf.nist.gov> (2025)
- [23] Temme, N.M.: *Special Functions: An Introduction to the Classical Functions of Mathematical Physics*. Wiley, Hoboken, NJ (1996)
- [24] MapleSoft: Maple 2015. <https://maplesoft.com> (2015)
- [25] Johansson, F., et al.: mpmath: a Python Library for Arbitrary-precision Floating-point Arithmetic. (2023). <http://mpmath.org>
- [26] Chen, J., Revels, J.: Robust Benchmarking in Noisy Environments.

<https://arxiv.org/abs/1608.04295> (2016)

Table 1: Sample from the tested dataset where Algorithm 644 skips calculations (hence, returns (0.0, 0.0)) due to very conservative overflow/underflow borders.

	ν	$\text{Re}(z)$	$\text{Im}(z)$	$ \epsilon_{\text{Re}} $	$ \epsilon_{\text{Im}} $
Point	45.203 537	5.198 871 592 860 476 8 $\times 10^{-6}$	3.246 113 018 266 729 1 $\times 10^{-6}$		
Maple		2.221 352 175 551 642 7 $\times 10^{-306}$	2.184 462 573 699 646 8 $\times 10^{-307}$		
Present		2.221 352 175 551 823 3 $\times 10^{-306}$	2.184 462 573 699 824 3 $\times 10^{-307}$	8 $\times 10^{-14}$	8 $\times 10^{-14}$
Alg. 644		0.0	0.0	1.0	1.0
Point	188.739 18	3.511 191 734 215 131 1	1.0 $\times 10^{-6}$		
Maple		1.062 602 688 129 752 0 $\times 10^{-303}$	5.712 854 682 321 659 2 $\times 10^{-308}$		
Present		1.062 602 688 129 822 9 $\times 10^{-303}$	5.712 854 682 322 039 6 $\times 10^{-308}$	7 $\times 10^{-14}$	7 $\times 10^{-14}$
Alg. 644		0.0	0.0	1.0	1.0
Point	788.046 28	1.0 $\times 10^3$	1.0 $\times 10^{-6}$		
Maple		2.761 094 516 724 992 1 $\times 10^{303}$	3.514 550 943 042 987 1 $\times 10^{297}$		
Present		2.761 094 516 725 014 6 $\times 10^{303}$	3.514 550 943 043 016 1 $\times 10^{297}$	8 $\times 10^{-15}$	8 $\times 10^{-15}$
Alg. 644		0.0	0.0	1.0	1.0
Point	788.0428	1.0 $\times 10^3$	1.2655 $\times 10^{-6}$		
Maple		2.761 094 516 723 647 $\times 10^{303}$	4.447 772 548 094 265 $\times 10^{297}$		
Present		2.761 094 516 723 669 $\times 10^{303}$	4.447 772 548 094 300 $\times 10^{297}$	8 $\times 10^{-15}$	8 $\times 10^{-15}$
Alg. 644		0.0	0.0	1.0	1.0